Hydrol. Earth Syst. Sci., 29, 159–177, 2025
https://doi.org/10.5194/hess-29-159-2025

Hydrology and Earth System Sciences
Open Access
EGU

Can system dynamics explain long-term hydrological behaviors? The role of endogenous linking structure

Xinyao Zhou[1], Zhuping Sheng[2], Kiril Manevski[3,4,5], Rongtian Zhao[6,7], Qingzhou Zhang[8], Yanmin Yang[1], Shumin Han[1], Jinghong Liu[1,9], and Yonghui Yang[1,4,9]

[1]Key Laboratory of Agricultural Water Resources, Hebei Laboratory of Agricultural Water-Saving, Center for Agricultural Resources Research, Institute of Genetics and Developmental Biology, Chinese Academy of Sciences, Shijiazhuang 050021, China
[2]Department of Civil Engineering, Morgan State University, Baltimore, MD 21251, USA
[3]Department of Agroecology, Aarhus University, Tjele 8830, Denmark
[4]Sino-Danish College, University of Chinese Academy of Sciences, Yanqihu Campus, Beijing 101408, China
[5]Department of Environmental Science, iClimate – Aarhus University Interdisciplinary Center for Climate Change, Roskilde 4000, Denmark
[6]State Key Laboratory of Resources and Environmental Information System, Institute of Geographic Sciences and Natural Resources Research, Chinese Academy of Sciences, Beijing 100101, China
[7]College of Resources and Environment, University of Chinese Academy of Sciences, Beijing 100049, China
[8]Land Resources Exploration Center of Hebei Bureau of Geology and Mineral Exploration and Development (Hebei Mine and Geological Disaster Emergency Rescue Center), Shijiazhuang 050081, China
[9]College of Advanced Agricultural Sciences, University of Chinese Academy of Sciences, Beijing 100190, China

Correspondence: Xinyao Zhou (zhouxy@sjziam.ac.cn) and Yonghui Yang (yonghui.yang@sjziam.ac.cn)

Received: 9 January 2024 – Discussion started: 29 January 2024
Revised: 29 October 2024 – Accepted: 14 November 2024 – Published: 14 January 2025

Abstract. Hydrological models with conceptual tipping bucket and process-based evapotranspiration formulations are the most common tools in hydrology. However, these models consistently fail to replicate long-term and slow dynamics of a hydrological system, indicating the need for model augmentation and a shift in formulation approach. This study employed an entirely different approach – system dynamics – towards more realistic replication of the observed slow hydrological behaviors at inter-annual and inter-decadal scales. Using the headwaters of Baiyang Lake in China as a case study, the endogenous linking structure of the hydrological system was gradually unraveled from 1982 to 2015 through wavelet analysis, Granger's causality test, and a system dynamics model. The wavelet analysis and Granger's causality test identified a negatively correlated and bidirectional causal relationship between actual evapotranspiration and catchment water storage change across distinct climatic periodicities, and the system dynamics approach suggested a combined structure of a vegetation reinforcing feedback and a soil water–vegetation balancing feedback in the hydrological system. The system dynamics' structure successfully captured the slow hydrological behaviors under both natural and human-intervention scenarios, demonstrating a self-sustained oscillation arising within the system's boundary. Our results showed that the interaction between the vegetation structure and the soil-bound water dominates the hydrological process at an inter-annual scale, while the interaction between the climatic oscillation and the soil-water-holding capacity dominates the hydrological process at an inter-decadal scale. Conventional hydrological models, which typically employ physiological-based evapotranspiration formulations and assume invariable soil characteristics, ignore vegetation structure change at the inter-annual scale and soil-water-holding capacity change at the inter-decadal scale, leading to failure in predicting the observed long-term hydrological behaviors. The system dynamics model is in its early stage with applications primarily confined to water-stressed regions and long-term scales. However, the novel

insights proposed in our study, including the different hierarchies corresponding to distinct mechanisms and timescales and the endogenous linking structure among stocks being a more important driver of the hydrological behaviors, offer potential solutions for better understanding a hydrological system and guidelines for improving the configuration and performance of conventional hydrological models.

1 Introduction

Hydrological models are scientific tools for describing and predicting the processes of the water cycle under the current and the future climate. In the simplest concept, a "bucket" is used to represent the water storage of a catchment, which is filled by rain and emptied by evaporation, transpiration, and streamflow (Fowler et al., 2020). In spite of the success of this concept in understanding the physical processes and revealing the physical parameters involved in hydrological events, such conventional hydrological models have performed poorly in simulating the long-term and slowly variable hydrological system observed in many regions across the world, e.g., the inter-annual cycles of catchment water storage (Creutzfeldt et al., 2012; Hulsman et al., 2021; Chang and Niu, 2023) and the multi-decadal decline of runoff (Chen et al., 2016; Peterson et al., 2021). Consistent inaccuracies of the conventional hydrological models in replicating slow hydrological behaviors suggest a lack of key mechanisms involved in the hydrological system. Alongside structural deficiencies (Fowler et al., 2020; Bouaziz et al., 2021), reasons for erratic model performance also include data errors (Kuczera et al., 2010; Hulsman et al., 2021), model structural deficiencies (Fowler et al., 2020; Bouaziz et al., 2021), poor parameterization (Fowler et al., 2016, 2018), or their combination. However, model structural deficiency likely plays a key role in most cases of poor performance (Fowler et al., 2020).

From a hydrological perspective, two main solutions have been proposed to improve the conventional hydrological model structure. The first introduces a "bottomless bucket" to avoid the "minimum possible storage" limit to the bucket, which empties the bucket on a seasonal basis and restricts the accumulation of water deficit (Fowler et al., 2020). The bottomless bucket configuration better tracks a long-term decline in soil moisture seen, for instance, in Australia during the 13-year "millennium" drought, desiccating catchments slowly and gradually (Fowler et al., 2021). On the other hand, groundwater usually responds slowly to rainfall variability, and the lag timescales are mediated by the hydrogeology of the aquifers and the soil physical characteristics (Hughes et al., 2012; Markovich et al., 2016). Thus, it has also been suggested that inter-basin groundwater flow should be incorporated in hydrological models through a new deeper groundwater reservoir to allow models to better reproduce long-term storage fluctuations (Bouaziz et al., 2018; Hulsman et al., 2021). Although some aspects are improved by these reconfigurations or modifications, other aspects of the hydrology behaviors are still not captured or reflected well, for instance those related to the effect of the terrestrial vegetation on the long-term and slow dynamics in hydrological models (Fowler et al., 2021).

The system dynamics approach assumes that ample time is required for a system to undergo changes (Meadows, 2008) and is thus a different approach to describe and interpret the mechanism of the ubiquitously long-term and slow variations of the hydrological system. Different from the conventional viewpoint postulating that the dynamics of a system are primarily driven by exogenous variables, the system dynamics approach seeks explanations of endogenous structure for the often complex, difficult-to-understand dynamics and "behaviors" (Forrester, 1968). This is because, on the one hand, stocks generally change slowly and thus can act as delays, lags, buffers, or shock absorbers in the system (Meadows, 2008). This characteristic is also prominent in the hydrological system and has been built into conventional hydrological models using various stocks (soil moisture/groundwater/lakes), leading to description of some slow hydrological dynamics (O'Connell et al., 2016). On the other hand, stocks are complexly linked with other even competing feedback loops operating simultaneously, creating counteracting and compensating pressures in response to exogenous disturbances (Richardson, 2020). Therefore, exogenous drivers might not be able to explain and anticipate a system's main pattern of behaviors, as the cause and the effect are often distant in time and space in dynamically complex systems (Davis, 2003). However, the complexity of linking structure among stocks has never been well recognized in conventional hydrological models, which often link these stocks simply and sequentially. The fact that stocks usually operate at different timescales further increases the complexity of linking structure among stocks in a hydrological system. In spite of the wide application of system dynamics in different areas (Wiener, 1948; Zera, 2002; Hofkirchner and Schafranek, 2011; Seth and Bayne, 2022), including land use dynamics (Lauf et al., 2012) and water management (Bai et al., 2021; Simonovic, 2020) in which the natural system only plays a minor role, to our knowledge, the concept has rarely been used in hydrology under natural conditions. The system dynamics approach may thus open a new avenue to understand the mechanisms of the long-term and slow dynamics of the hydrological system.

By means of the system dynamics approach, the main aim of this paper was twofold, to (1) seek the explanation of endogenous linking structure among stocks for the long-term and slow hydrological dynamics with a case study and (2) test the ability of the endogenous linking structure for (re)producing and predicting long-term and slow hydrological dynamics. To make the discussion clearer, the "long term" is constrained to the following. As a complex system,

a hydrological system comprises multiple hierarchies. Each hierarchy is governed by a distinct mechanism and produces fluctuations/cycles at a certain timescale. Notably, the time series yielded in each hierarchy can be considered long-term or "slow" compared to its predecessor. Here, we define that a low hierarchy corresponds to the intra-annual scale, a high hierarchy corresponds to the inter-annual scale, and an even higher hierarchy corresponds to the inter-decadal scale. This definition has been inspired by a previous study, of which results showed that a clayey-soil catchment tends to exhibit higher flow in the short term but less discharge in the long term than its sandstone counterpart, indicating distinct underlying mechanisms to control streamflow generation at different hierarchies/timescales (Xiao et al., 2019), as well as a study which proposed a fill–spill phenomenon across scales (McDonnell et al., 2021). Considering the objectives of this study and the data span, we specify the long term as inter-annual to inter-decadal scales.

2 Methodology

2.1 Study site description

The study area was located at Taihang Mountain in northern China and comprised of the catchments of the rivers Sha, Tang, and Juma (Fig. 1). The climate is semi-arid with continental monsoons, i.e., hot, humid summers and cold, dry winters. The average annual temperature, precipitation, and potential evapotranspiration are 7.5 °C, 556 mm, and 1369 mm, respectively (Yang and Mao, 2011; Zeng et al., 2021). Rainfall is the main source of streamflow in the study area (Fu et al., 2024). The main geologic characteristics of the Taihang Mountain area are "soil and rock dual texture", with thin topsoil of 0.2–0.5 m rich in plant roots and gravel and a thick 0.5–10 m subsoil of weathered granite gneiss with highly developed fractures (Cao et al., 2022). The soil of Taihang Mountains is primarily developed from granite, gneiss, limestone, and sandstone. Cambisols and Luvisols constitute the dominant soil types, accounting for 46.86 % and 15.46 % of the total area, respectively (Fu et al., 2021). These soil types all have a high content of sand gradation, approximately 50 %, followed by silt. Clay comprises the smallest proportion of the soil content, at approximately 20 % (Yang and Cao, 2021). The three rivers flow into Baiyang Lake, the largest freshwater lake in the North China Plain (Zhuang et al., 2011). Due to prolonged droughts and intensive human interference since the 1980s, the amount of inflow water to the lake has decreased significantly (Fig. S1 in the Supplement). This has resulted in a continuous shrinkage of the water body and ecological degradation in the lake area (Han et al., 2020). Despite many efforts quantifying the impacts of climate change and human activities on the dramatic runoff reduction (Zhuang et al., 2011; Hu et al., 2012; Wang et al., 2021), there have not been many studies that have investigated the dynamics of the catchment water storage in the study area (Chaffaut et al., 2022; Huang and Yeh, 2022).

2.2 Data compilation and pre-processing

Yearly streamflow, rainfall, and actual evapotranspiration data spanning the years 1982–2015 period were compiled for the catchments. Streamflow (Q) from four hydrological stations, viz. Fuping (FP), Daomaguan (DMG), Zijingguan (ZJG), and Zhangfang (ZF), were acquired from the Department of Water Resources of Hebei Province (hereafter the names of the gauge stations are used for representing the catchments; Fig. 1). The FP station is located in the Sha River catchment with a drainage area of 2160 km^2, whereas DMG station is located in the Tang River catchment with a drainage area of 2704 km^2. ZJG and ZF are the upstream and the downstream stations of the Juma River, respectively, with corresponding drainage areas of 1751 and 4737 km^2. The unit of streamflow data was $m^3\ s^{-1}$ in the original dataset and was converted to $mm\ yr^{-1}$ by dividing by the area.

Precipitation data (P; $mm\ yr^{-1}$) from 34 national weather stations within the study area were downloaded from the China Meteorological Data Sharing Service System (http://data.cma.cn/, last access: 9 January 2025). Actual evapotranspiration (AET; $mm\ yr^{-1}$) from 1982 to 2015 was the average of two gridded remote-sensing-based AET products, the Numerical Terradynamic Simulation Group (NTSG; https://www.umt.edu/numerical-terradynamic-simulation-group/default.php, last access: 9 January 2025; 8 km spatial resolution) and ETWatch (8 km resolution for 1984–1989 and 1 km for 1990–2015). The AET data for the first 2 years were taken from NTSG and those of 1984–2015 were taken from ETWatch. ETWatch (http://etwatch.cn/html/datasetdatail.html?id=33333a2bee794dac99bc22ec626f430d, last access: 9 January 2025) uses the Penman–Monteith model integrated with the SEBAL and the SEBS models (Wu et al., 2008, 2021), and previous studies show reliable ET estimates over the Haihe Basin where the study area is located (Moiwo et al., 2011; Wu et al., 2012). The NTSG is also a Penman–Monteith model (Zhang et al., 2009, 2010). Furthermore, two alternative AET products, CR (complementary-relationship-based modeling, Ma et al., 2019a, b) and PEW (proportionality hypothesis-based surface energy-water balance model, Fu and Wang, 2022; Fu et al., 2022), were taken for cross-validation with ETWatch and NTSG. Complementary-relationship and Priestley–Taylor approaches were employed by CR and PEW, respectively. Despite their algorithmic difference, the four AET products exhibit comparable values and common characteristics (Fig. S2). Firstly, all products successfully captured the annual AET fluctuations. Secondly, in terms of long-term trends, all products indicated a decline in AET at the end of 1990s and the beginning of 2000s. While AET data of NTSG and ETWatch showed an upward trend thereafter,

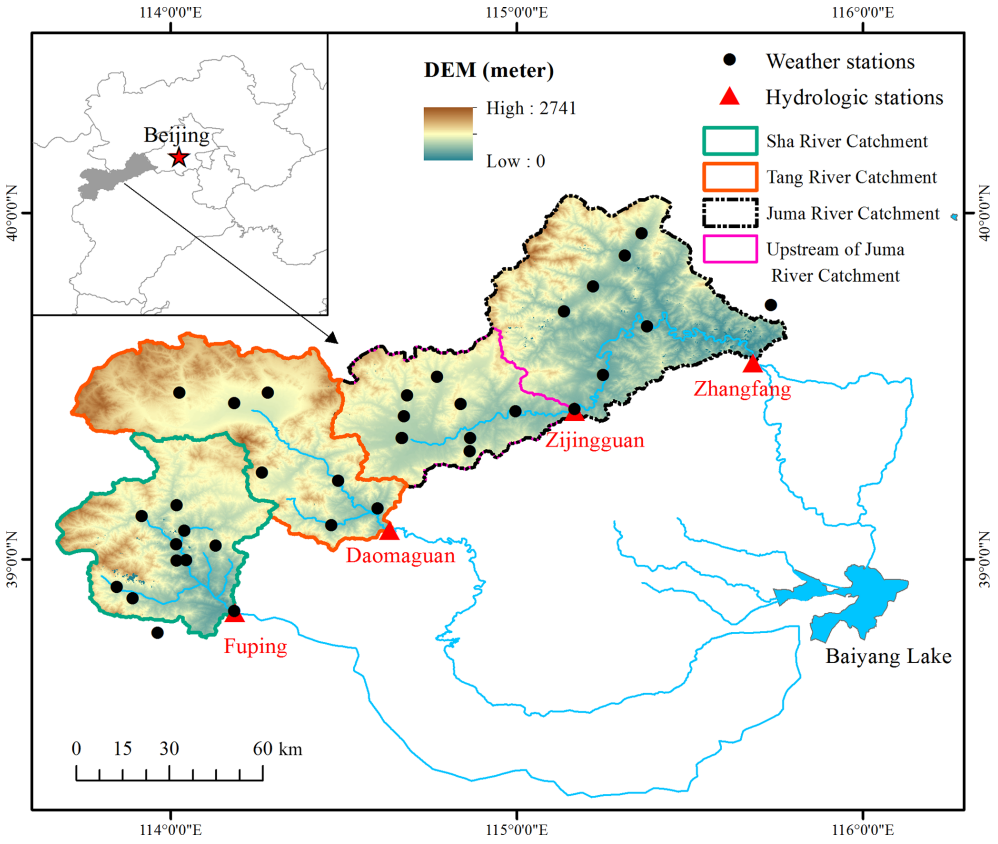

Figure 1. The location of the study area in China at Baiyang Lake and its headwaters.

AET data of CR and PEW continued to decrease during the study period. Thirdly, the magnitude of fluctuations of P and Q reduced in the later stage. Given these observations, we conclude that the ETWatch product demonstrates reliable values and the most distinguishable pattern among the four AET products; thus it was deemed a reliable choice for AET estimation.

Catchment water storage change (ΔS; mm yr^{-1}) was calculated by the mass balance method subtracting streamflow and actual evapotranspiration from precipitation ($\Delta S = P - Q - \mathrm{AET}$). Detrended total water storage anomaly (TWSA; mm yr^{-1}) and surface soil moisture (SM; m^3 m^{-3}) data were used for comparison with ΔS. The TWSA data were based on reconstructed GRACE/GRACE-FO global surface mass changes (land + ocean) from 1979 to 2020 at 0.5° spatial resolution (Li et al., 2021). Surface SM data with a spatial resolution of 0.25° and temporal coverage from 1979 to 2020 were downloaded from the European Space Agency Climate Change Initiative (ESA CCI) website (Dorigo et al., 2017, https://climate.esa.int/en/data/#/dashboard, last access: 9 January 2025). This dataset had a high outperformance among satellite-based products (Ma et al., 2019c). Comparison of the three datasets is shown in Fig. S3.

Land use data for the Haihe Basin for the 1980s, 1990s, 2000s, and 2010s at 30 m spatial resolution were obtained from the ETWatch (http://etwatch.cn/html/datasetdatail.html?id=79f37dea8d0c42cf82390bf0a94a59e7, last access: 9 January 2025) website. From 1980s to 2010s, arable land and high-coverage forest land kept decreasing, while low-coverage vegetation greatly increased after 2000s (Fig. S4).

Future monthly rainfall ("pr" in CMIP), monthly total runoff ("mrro" in CMIP), and AET ("evspsblsoil" and "evspsblveg" in CMIP), stemming from three scenarios (SSP126, SSP245, and SSP585) within four global climate models (GCMs; ACCESS-CM2, CNRM-ESM2, EC-Earth3, and GFDL-CM4), were retrieved from CMIP6 (phase 6 of the Coupled Model Intercomparison Project, https://esgf-node.llnl.gov/search/cmip6/, last access: 9 January 2025), covering the time span from 2015 to 2100. Notably, the GFDL-CM4 model lacks the SSP126 experiment, and the ACCESS-CM2 model lacks the evspsblveg variable. The spatial resolution varies, with 250 km for ACCESS-CM2 and CNRM-ESM2 models and 100 km for EC-Earth2 and GFDL-CM4 models. The grid values corresponding to the study area were extracted. For ACCESS-CM2 (CNRM-ESM2), the grid value at the 62nd (83rd) row and 104th (93rd) column, corresponding to longitudes of 115.3125° (115.3125°) and latitudes of 39.375° (39.9218°), were used. Similarly, for EC-Earth3 (GFDL-CM4), the grid values at the 164th (92nd) and 165th (93rd)

rows and the 185th (130th) column, corresponding to longitudes of 114.6094° (114.375°) and 115.3125° (115.625°), and latitudes of 39.649° (39.5°), were utilized. The unit of $\mathrm{kg\,m^{-2}\,s^{-1}}$ was converted to millimeters per month by multiplying it by 86 400 s and 30 d. Subsequently, annual values were calculated by summing the monthly values. The annual rainfall was averaged from four GCMs and used to drive the system dynamics (SD) model, generating Q and AET estimates under different SSP scenarios.

2.3 Formal data analysis

We propose three approaches – wavelet analysis, Granger's causality test, and system dynamics. Although some information about the endogenous linking structure of hydrological system can be inferred from the wavelet analysis and Granger's causality test, additional knowledge from multiple subjects is necessary to build the system dynamics' structure. For example, considering vegetation growth to be a reinforcing feedback loop requires collective prior knowledge of plant physiology (Lian et al., 2021; Wright and Francia, 2024), resource competition theory (Craine and Dybzinski, 2013), population ecology (Snider and Brimlow, 2013), and likely other knowledge not included in this study. Therefore, the proposed three approaches run in parallel and are not sequential to help us understand the endogenous linking structure among the stocks in the hydrological system.

2.3.1 Wavelet analysis

The continuous wavelet transform (CWT) was employed to preliminarily identify connection patterns among variables in the time series. The wavelet transform has emerged as one of the most promising function transformation methods acting as a time and frequency localization operator (Pathak, 2009). The advantage of the wavelet transform is that it can reflect the evolution over time of non-stationary time series. Here the CWT analysis was used to generate varying coefficients that signify the similarity between the signal and mother wavelets at any specific scale base. The CWT of a function f with respect to the mother wavelet Ψ is defined by Pathak (2009):

$$W_f(a,b) = \frac{1}{\sqrt{|a|}} \int f(t)\Psi\left(\frac{t-b}{a}\right) \mathrm{d}t, \tag{1}$$

where $W_f(a,b)$ is the wavelet coefficient, a is the wavelet scale associated with dilation and contraction of a wavelet, and b is a time index describing the location of the wavelet in time. Ψ is known as "mother" wavelet because it can generate "child" wavelets by dilation and translation. The function is then processed with these child wavelets to yield the wavelet coefficient (Sayood, 2012).

Prior to the analysis, the time series data of P, AET, Q, and ΔS were standardized by subtracting the mean and dividing the standard deviation. Afterwards, correlation analysis was conducted based on the CWT coefficients. A contraction parameter of 8 was used in this study as the highest for the wavelet power spectrum of multi-decadal periodicities (Fig. S5).

2.3.2 Granger's causality test

Granger's causality test was adopted to decide the causal direction of connections among variables. Correlation analysis alone can only tell how "similar" two variables are; however, correlation is neither necessary nor sufficient condition for causality (Sugihara et al., 2012). Inferring causal direction is important for understanding how a complex system works. Granger's causality test is a widely used method to investigate causality between two variables in a time series (Stokes and Purdon, 2017; Shi et al., 2022). For two time series from processes X and Y, it can be said that X does not Granger-cause Y if X, conditional on its own past, is independent of the past of Y (Banerjee et al., 2023). The typical method to test this dependency of two time series involves fitting a vector autoregressive model for X and measuring whether inclusion of Y in that model makes the fitting error significantly lower:

$$y_i = \alpha_0 + \sum_{j=1}^{m} \alpha_j y_{i-j} + \sum_{j=1}^{m} \beta_j x_{i-j} + \varepsilon_i, \tag{2}$$

where α_j and β_j are the regression coefficients and ε_i is the error term. The test is based on the null hypothesis.

$$H0 : \beta_1 = \beta_2 = \ldots == \beta_m = 0.$$

The X Granger-causes Y when the null hypothesis is rejected.

Further details on the theory behind Granger's causality test and the MATLAB toolbox used in this work can be found in Robert (2023).

2.3.3 System dynamics approach

Causal structure is different from the system dynamics' structure due to the lack of "feedback" concept in causal inference. Feedback is in the core of the system dynamics concepts (Meadows, 2008; Richardson, 2020). A feedback loop exists when information resulting from certain actions eventually returns in some form, potentially influencing future actions (Richardson, 2020). Feedback loops can be reinforcing or balancing, the former aiming for exponential growth or accelerating collapse, as disequilibrating and destabilizing structures in systems, and the latter aiming for stability and resistance to change, for equilibrating or goal-seeking structures in the system (Meadows, 2008). Combined, reinforcing and balancing feedback loops can generate all manners of dynamic patterns. The inference of feedback loops should be from prior experience. Both feedback loops coexist in the case study. The reinforcing feedback loop can be considered to be the change of vegetation structure because the processes

tend to self-enhance once they have started. Here, the vegetation structure includes non-physiologic components, e.g., change in composition by growth and mortality (Li et al., 2023). For example, vegetation growth will create a more humid environment for the benefit of its further growth, while vegetation mortality will exacerbate deterioration and trigger a "death spiral" (Bruelheide et al., 2018). Soil moisture, on the other hand, can interrupt the self-enhancing processes of change in vegetation structure and is thus considered a balancing feedback loop. For example, soil moisture approaching the wilting point increases the difficulties of the root to absorb water, causing slower and finally stagnant vegetation growth, and vice versa (Stocker et al., 2023).

How does the interplay between soil moisture and vegetation structure drive the dynamics of the hydrological system at the inter-annual scale? Firstly, every balancing feedback loop has a desired goal used to compared to the actual system state. If a stock level is above or below the goal, the discrepancy between the actual and the desired levels will initiate corrective action and bring the state of the system back in line with the goal. Here the desired soil moisture was considered a value within the range between field capacity and wilting point because in this range water can be held in soil and used for vegetation absorption. Secondly, while traditional hydrological models usually use exogenous variables to calculate AET using physical-process-based models such as the Penman or the Thornthwaite models, the system dynamics approach calculated AET based on its earlier value. This is because there was an implicit vegetation structure stock behind AET. Starting with an initial vegetation structure level, the growth of new vegetation can be shown as an inflow and mortality of old vegetation as an outflow, which would also drive smooth transformation of AET. Since vegetation structure stock can remember the history of changing flows and the growth/mortality of vegetation generally took several years, AET gradually changed and showed increase or decrease cycles at the inter-annual scale. The equations of the dynamics of hydrological system solved for each year from 1982 to 2015 are as follows:

$$\mathrm{TWS}(t) = \mathrm{SMS}(t) + \mathrm{GWS}(t) + \mathrm{SWS}(t) \tag{3}$$

$$\mathrm{SMS}(t) = \mathrm{SMS}(t-1) + \Delta s(t) \cdot \mathrm{DT} \tag{4}$$

$$\Delta s(t) = [(P(t) - Q_\mathrm{r}(t)] - \mathrm{AET}(t) - \mathrm{RCH}(t) \tag{5}$$

$$\mathrm{DISC}(t) = [\mathrm{SMS}(t-1) - \mathrm{ESMS}]/\mathrm{DT} \tag{6}$$

$$Q_\mathrm{r}(t) = [P(t) + \mathrm{DISC}(t)] \cdot \mathrm{C1} \tag{7}$$

$$\mathrm{AET}(t) = \mathrm{AET}(t-1) + [\mathrm{VEG}(t) + \mathrm{DISC}(t)] \cdot \mathrm{C2} \tag{8}$$

$$\mathrm{RCH}(t) = [P(t) \cdot \mathrm{C3} + \mathrm{DISC}(t)] \cdot K(t) \tag{9}$$

$$Q_\mathrm{s}(t) = \mathrm{GWS}(t-1) \cdot \mathrm{C4}/\mathrm{DT} \tag{10}$$

$$\mathrm{GWS}(t) = \mathrm{GWS}(t-1) + \mathrm{RCH}(t) \cdot \mathrm{DT} - Q_\mathrm{s}(t) \cdot \mathrm{DT} - \mathrm{GP}(t) \cdot \mathrm{DT} \tag{11}$$

$$\mathrm{SWS}(t) = [Q_\mathrm{r}(t) + Q_\mathrm{s}(t)] \cdot \mathrm{DT}, \tag{12}$$

where TWS, SMS, GWS, and SWS are, respectively, total water stock, soil moisture stock, groundwater stock, and surface water stock (all in mm); Δs is the change in water in soil moisture stock (in mm yr^{-1}); DISC (in mm yr^{-1}) is the discrepancy between actual (SMS) and desired (expected) soil moisture stock (ESMS; mm); and P is precipitation inflow (in mm yr^{-1}), whereas AET, RCH, Q_r, and Q_s are outflows indicating, respectively, actual evapotranspiration, recharge, rapid-response runoff, and slow-response runoff (mm yr^{-1}). VEG and GP are human activity parameters for, respectively, vegetation-related activities such as reforestation, and groundwater pumpage (both in mm yr^{-1}), with their value of 0 representing no human influence. C1, C2, C3, and C4 are dimensionless coefficients with physical interpretations of, respectively, proportion of impermeable area, proportion of soil bound water utilization by AET, proportion of rainfall into deeper layer, and proportion of outflowing groundwater. K is dimensionless response coefficient related to intrinsic permeability and determined by soil type only, and DT is time interval of 1 year in this study. The choice of the time interval is due to both the study's purpose and the fact that mean travel time of a non-groundwater-dominant catchment is around 1 year or slightly longer, leading to catchment soil water stock typically updates at an annual step (Jutebring Sterte et al., 2021). The initial values of parameters are first obtained from the literature and then calibrated against observed AET and Q.

3 Results

3.1 Preliminary identification of interconnection pattern

The wavelet analysis revealed significant periodicities in the precipitation data for the study area in the 7th–8th and 14th–15th years of the 1982–2015 period (Fig. S5). The periodicities were consistent with those of the Pacific Decadal Oscillation (PDO), which is the prime driver of inter-decadal change

in summer rainfall over eastern China (Nalley et al., 2016; Zhu et al., 2015). Here we divide the whole study period into two distinct phases – wet and dry. Firstly, from a climatic perspective, this is because the PDO phase has shifted from a positive to a negative mode since the late 1990s, corresponding to the decrease in rainfall in the study area (Fig. S6). Meanwhile the self-calibrating Palmer Drought Severity Index (SC-PDSI) and the Standardized Precipitation Evapotranspiration Index (SPEI) calculated from the climatic data in Beijing, China, both showed major dry periods in 1980–1985 and 1999–2011 (Zhao et al., 2017). Secondly, in terms of streamflow, streamflow of the headwater of Baiyang Lake significantly decreased, with a tipping point in around 2000 (Fig. S7; Cui et al., 2019; Xu et al., 2019), although precipitation does not show a significant trend (Fig. S8). Thirdly, according to wavelet analysis, a dampening process in the magnitude of fluctuations in the wavelet coefficients was identified for P and Q after 2000. All this information indicated that the hydrological system transitioned from a wet phase to a dry phase around 2000. The wet phase started in 1984 and ended in 2000, while the dry phase was from 2001 to 2015.

Figure 2 shows the comparison of the four signals (P, AET, Q, and ΔS) in the four catchments of the study area. The P signal in the four catchments regularly fluctuated in the wet phase, while dampening fluctuations appeared in the dry phase with weaker amplitudes and lower frequencies. The Q signal was roughly synchronous with the P signal, with similar amplitude and frequency. The ΔS signal showed in-phase connection with P signal in the wet phase; however, the in-phase connection disappeared in the dry phase. The AET signal was out of phase with the other signals in the wet phase, while in the dry phase, AET signal only opposed the ΔS signal in their phases.

The correlation analysis (Fig. 3) corroborated the preliminary interconnection results observed in the wavelet analysis, both for the entire study period and the dry-/wet-phase period. The AET signal was significantly and negatively correlated with the other signals in the wet phase but only with the ΔS signal in the dry phase. The Q signal significantly and positively correlated to P signal in both dry and wet phases. The ΔS signal in the wet phase showed significant positive correlations with P and Q signals while negative correlation with AET signal in wet phase. In the dry phase, the ΔS signal was significantly negatively correlated only to the AET signal. Comparable correlations were observed for all four catchments, with larger and more significant values (e.g., ΔS versus AET) for FP and DMG catchments than ZJG and ZF.

3.2 Development of endogenous linking structure of the hydrological system

The causal relationships among variables play an important role in helping to understand the endogenous linking structure of a hydrological system. Taking the FP catchment as an example (Fig. 4), Granger's causality test showed that P does not Granger-cause AET, while it does Granger-cause Q and ΔS; AET does not Granger-cause Q, while it Granger-causes ΔS; and ΔS Granger-causes Q and AET. The bidirectional causal relationship between ΔS and AET denotes the existence of unobserved common variables, referred to as confounders (Pearl, 2009; Morgan and Winship, 2015). According to the theory of causal inference, confounders can obscure or blur the "real" causal relationship; thus it is advisable to establish subgroups to analyze the causal relationship separately. In the context of our study, the causal relationship of ΔS and AET is "confounded" by soil water: AET causes ΔS when soil water is plentiful, whereas ΔS causes AET when soil water is scarce.

The endogenous linking structure of the hydrological system based on Granger's causality test was built in a three-step procedure. First a complete undirected graph is constructed (Fig. 5a), followed by elimination of edges between variables that are independent, in this case the edges between AET and P and between AET and Q (structure shown in Fig. 5b), and finally a direction of the adjacent edges is provided according to the results (Fig. 5c). However, additional knowledge is necessary to identify the reinforcing/balancing feedback loops and to form the system dynamics' structure of the hydrological system. As shown in Fig. 5d, the main trait of the structure built using the system dynamics approach is the soil–vegetation feedback to drive the system's dynamic equilibrium, while P was input and Q was influenced by the soil–vegetation feedback structure.

The most interesting knowledge that the system dynamics' structure depicted was that the boundary of the hydrological system should be expanded to incorporate AET (vegetation structure) as an endogenous variable. According to system dynamics theory, exogenous variables should have no feedbacks from or interactions with the stocks inside the system boundary (Sterman, 2000). For this study, it was appropriate to exclude P outside the system boundary and consider P the sole source variable because P was insensitive to AET and SM over small area (Wei and Dirmeyer, 2019). Meanwhile, AET (vegetation structure) exhibited strong interactions with SM. Therefore, AET (vegetation structure) should be included as an endogenous variable. Over an inter-annual timescale, AET (vegetation structure) was SM-dependent and played an important role in maintaining the dynamic equilibrium of SM. The outflow rate of AET (vegetation structure) could be higher under ample soil water while lower under a lack of soil water. Treating AET (vegetation structure) as an exogenous variable may lead to inappropriate depletion rate of SM, as current AET (vegetation structure) was often not related to current climate, which in turn caused further miscalculations of hydrological variables in subsequent periods. Currently, the AET estimation is based on a remote-sensing-based vegetation index, which, however, makes the predictions of future AET impossible because the future vegetation index cannot be obtained. Additionally, rapid-response runoff and slow-response runoff were consid-

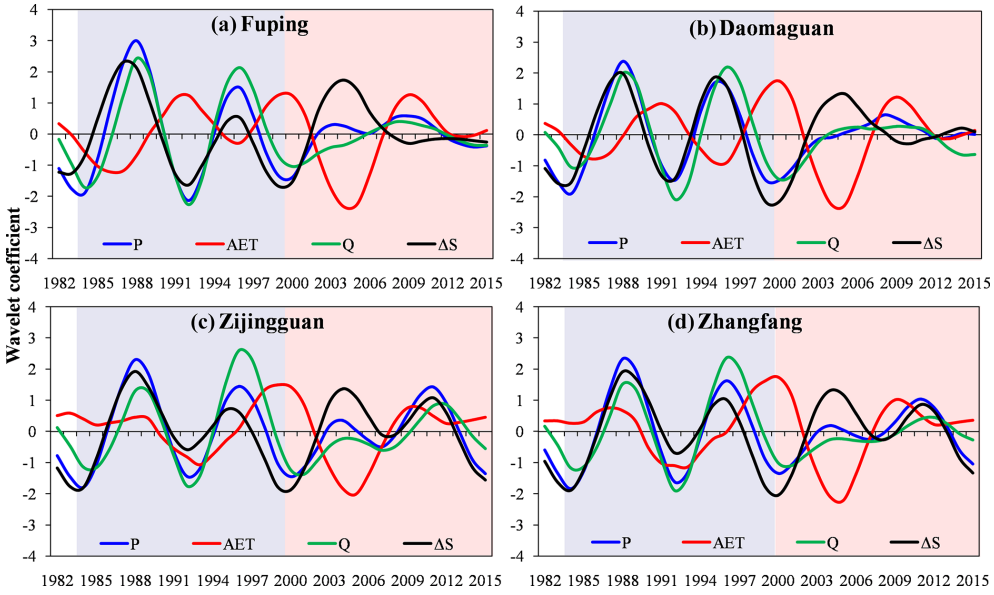

Figure 2. Wavelet coefficients of four signals (precipitation, P; actual evapotranspiration, AET; streamflow, Q; and catchment water storage change, ΔS) with a contraction parameter of 8 in the Fuping catchment **(a)**, Daomaguan catchment **(b)**, Zijingguan catchment **(c)**, and Zhangfang catchment **(d)**. The blue background indicates the wet phase from 1984 to 2000, while the red background indicates the dry phase from 2001 to 2015.

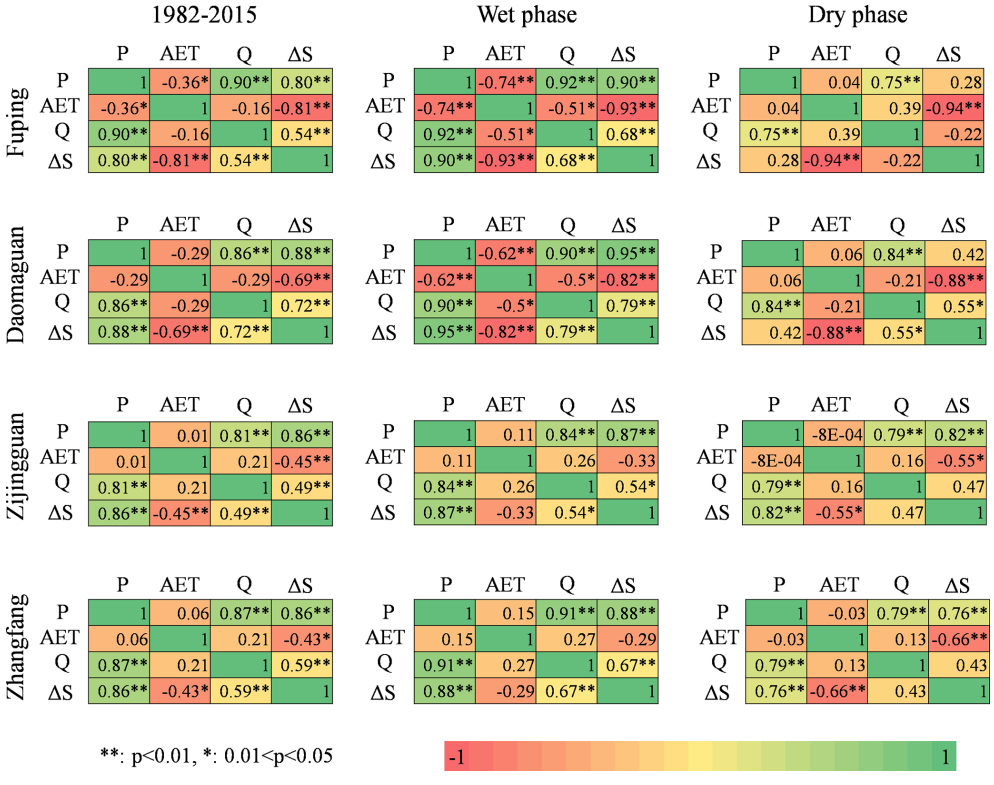

Figure 3. Pearson's correlation matrices for four variables for the whole study period, the wet phase and the dry phase. The calculation is based on wavelet coefficients with a contraction parameter of 8.

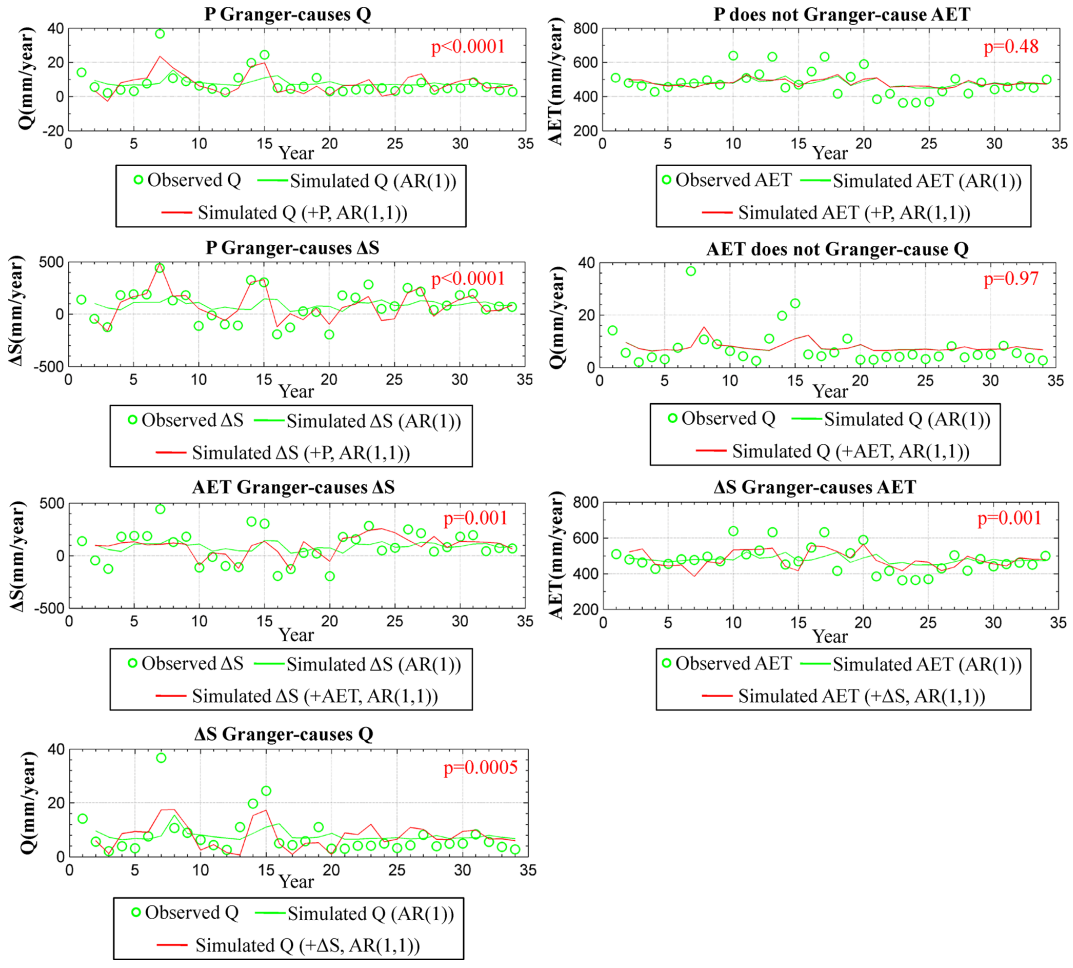

Figure 4. Causal relationships among four hydrological variables of the FP catchment. P, Q, AET, and ΔS indicate rainfall, streamflow, actual evapotranspiration, and catchment water storage change,, respectively. AR(p) represents the autoregressive model, where "p" is called the order of the model and represents the number of lagged values we want to include. AR(p, q) represents that the additional q-order variable is included. The p value indicates significance at 95 % confidence. Comparable results of Granger's causality test were seen for the other catchments (not shown for clarity purposes).

ered sink variables of the hydrological system because their influence on SM and AET could be disregarded once they had coalesced into the riverbed.

3.3 Dynamics simulation of the hydrological system

According to the system dynamics equations (Eqs. 3–12), using observed P as input and starting with an initial soil moisture state, the dynamics of AET, Q, ΔS ($= P - \mathrm{AET} - Q$), and TWS (total water storage = soil moisture + groundwater + surface water) were simulated for the FP catchment as an example under both natural and human activity scenarios (Fig. 6). Here AET1, $Q1$, $\Delta S1$, and TWS1 represent the simulated values with constant ESMS, while AET2, $Q2$, $\Delta S2$, and TWS2 represent the simulated values with varying ESMS. Under a natural scenario (GP = 0, VEG = 0), with a constant ESMS value, the simulated AET captured the inter-annual cycles during the study period, despite the lack of annual fluctuations. Simulated Q and ΔS captured both the annual fluctuations and the inter-annual cycles (the R^2 values of simulated AET, Q, and ΔS are 0.19, 0.21, and 0.82, respectively). However, the discrepancies between observed and simulated AET and ΔS increased over time. If different climatic phases were considered and varying ESMS was adopted to reflect the shift of climatic phase over decadal scale (lower ESMS from 1982–2000 and higher ESMS from 2001–2015), the discrepancies became smaller (the R^2 values of simulated AET, Q, and ΔS were 0.33, 0.17, and 0.85, respectively).

Evident from Fig. 6 was the increase in simulated total water storage after 2000 against an observed anomaly decrease, which was probably caused by human interventions not reflected in the simulation such as groundwater overexploitation and afforestation activity in the study area since 2000, also seen in the increase in the regional normalized difference

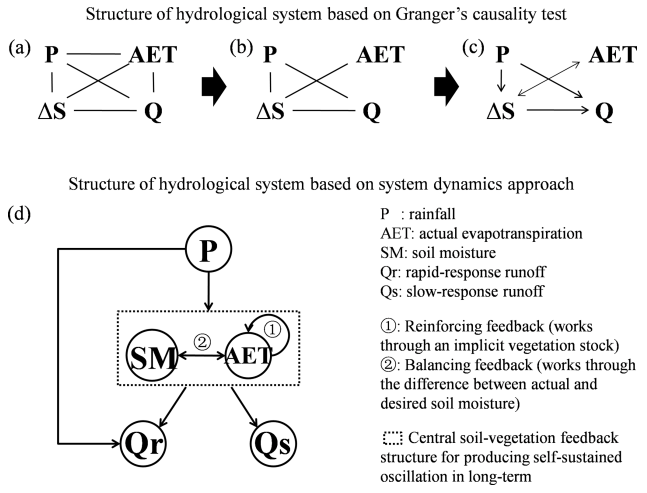

Figure 5. The comparison of endogenous linking structures of hydrological system built using two approaches, Granger's causality test and the system dynamics approach. **(a–c)** Illustration of how the structure built using causal analysis and **(d)** structure built using the system dynamics approach.

vegetation index (NDVI; Fig. S9). Both observed data and a literature review were used to set up human activity scenarios. Firstly, given the lack of groundwater pumpage data for the study area and the time frame, we estimated it based on the existing literature. The water use of the household sector in the county of FP mainly relies on groundwater, and water demand is projected to increase in the future (Wei and Wang, 2019). Furthermore, the groundwater depletion or the decline of water table in North China Plain also showed an exponential increase during the study period (Gong et al., 2018; Lancia et al., 2022; Huang et al., 2023). Secondly, NDVI data showed a linear upward trend during the majority of the study period (Fig. S9), and the literature showed that the Taihang Mountains Afforestation Project launched in 1987 and the coverage of vegetation increased 11.2 % from 1994 to 2013 (Hu et al., 2017, 2019; Yuan et al., 2019). Therefore two human-intervention scenarios were assumed to linearly increase AET and exponentially increase groundwater pumpage. When the groundwater pumpage scenario was introduced, the simulated AET, ΔS, Q, and TWS all greatly improved. When the afforestation scenario was added, it further pushed all the simulated values closer to the observations (the R^2 values of simulated AET, Q, and ΔS increased notably to 0.35, 0.30, and 0.86, respectively).

Simulations were conducted for the other three catchments with same initial values, parameters, and scenarios (Figs. S10–S12). Despite small discrepancies caused by the parameterization, for instance, the overestimated Q in the ZF catchment, the inter-annual cycles were captured well in all catchments, indicating the robustness of the system dynamic approach. It is thus important to note that the system dynamics approach was insensitive to initial values of variables. In addition, the divergence between observed TWSA and simulated TWS in the first several years was probably caused by the inaccurate reconstruction of TWSA series because TWS was less likely decreasing under a humid climate and marginal groundwater pumpage.

Using the system dynamics' structure, we computed future runoff and AET from 2015 to 2100 under different SSP + RCP scenarios and compared the results with those from four GCMs (Fig. 7). In terms of AET, the system dynamics' structure aptly captured its primary behavioral patterns: a decline in the 2040s and 2070s, followed by an increase in the 2060s and 2090s. Notably, the R^2 values between system dynamics' results and GCMs' results were relatively higher for SSP585, specifically 0.48 for ACCESS-CM2, 0.15 for CNRM-ESM2, and 0.41 for EC-Earth2 but 0.04 for GFDL-CM4. For the other two SSPs, the R^2 values were relatively poor. Regarding runoff, the system dynamics' simulations indicated an increasing trend, whereas the GCMs' estimation did not exhibit any discernible trend. The R^2 values between system dynamics' results and GCMs' results for runoff were poor across all experiments. These findings further emphasized the fact that the system dynamics' structure is capable of producing long-term hydrological behaviors. Conversely, while adept at capturing short-term fluctuations, process-based models fall short in simulating long-term hydrological behaviors due to a lack of structure.

4 Discussions

4.1 Distinct mechanisms in different hierarchies of a hydrological system

Here we discuss the interpretation of the underlying mechanisms in terms of the hierarchies we defined in the hydrological system. In the lowest hierarchy, hydrological processes are primarily controlled by the interaction between rainfall density and sink-filling/macropore flow (McDonnell et al., 2021), which was conceptualized as a small, active reservoir (Xiao et al., 2019). At this level, soil properties, particularly non-capillary pores in the top layer, are predominant and a direct factor influencing the storage–discharge relationship at the intra-annual scale. In the higher hierarchy, hydrological processes primarily involve the interaction between vegetation structure change and soil bound water, defined as water stored in capillary pores (Good et al., 2015); this was conceptualized as a large, passive reservoir (Xiao et al., 2019). At this level, soil capillary pores in the deep layer become predominant and direct influencing factor. Water stored in capillary pores is primarily utilized by vegetation, further strengthening the link between vegetation and hydrological behaviors at the inter-annual scale. Ascending to an even higher hierarchy, the interaction between climatic oscillation and soil-water-holding capacity takes over the priority of a hydrological system to generate inter-decadal-scale

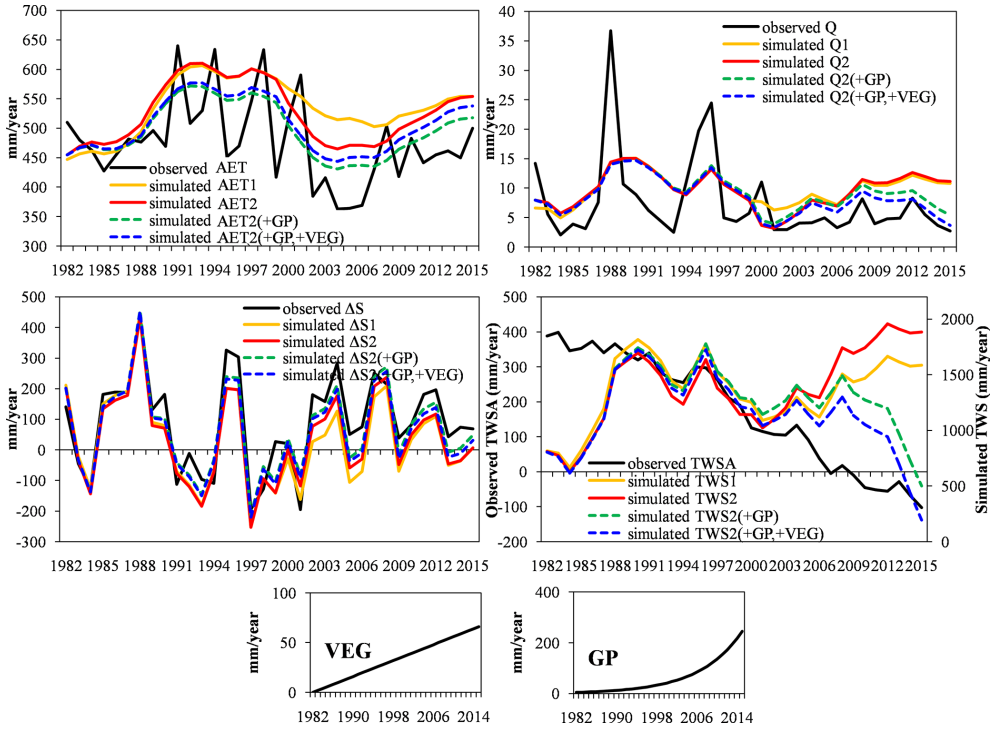

Figure 6. Observed and simulated actual evapotranspiration (AET), streamflow (Q), catchment water storage change (ΔS), and total water storage (TWS) using a system dynamics approach for the FP catchment. Yellow and red lines indicate the simulation without human interventions (GP = 0 and VEG = 0), with, respectively, fixed and varying desired soil moisture (ESMS). The dashed green line indicates simulation with groundwater pumpage (GP), which increased at an exponential rate. The dashed blue line is the simulation with GP and vegetation change (VEG), which is increasing at a linear rate. AET1, $Q1$, $\Delta S1$, and TWS1 represent the simulated values with constant ESMS, while AET2, $Q2$, $\Delta S2$, and TWS2 represent the simulated values with varying ESMS. TWSA is the anomaly of total water storage.

hydrological dynamics. This is because soil-water-holding capacity can be enhanced by the interplay of soil physical, chemical, and biological components during drought (Delgado and Gómez, 2016). Physically, drought alters aggregate size fraction with fewer macro-aggregates and more micro-aggregates (Zhang et al., 2019; Su et al., 2020). Also, pore network connectivity decreases due to reduced vegetation growth (Negassa et al., 2015), which likely increases soil-water-holding capacity under drought conditions because of a poorly connected soil pore network and the larger water-holding capacity of micropores (Patel et al., 2021). Chemically, the ionic strength of the soil solution can be up to 9 orders of magnitude greater in dry soils compared to saturated soils, creating extremely different chemical environment (Patel et al., 2021). This can cause desorption of different carbon molecules from minerals and soil organic carbon (SOC) destabilization (Bailey et al., 2019). Biologically, drought stress reduces the population and activity of soil animals and microbes. This can also destabilize SOC because the microbial community would preferentially consume the more labile/biodegradable organic molecules, leaving behind a more uniform, stable SOC pool (Kaiser et al., 2015). Furthermore, rainfall pulses in a drought period would drive water deeper because rainfall in dry spells usually occurs as discrete events (Manzoni et al., 2020). This makes it easier for water to be trapped by soil particles rather than utilized by plants, further decreasing evapotranspiration.

The lack of mechanisms in higher hierarchies in conventional hydrological models leads to their hierarchy at the intra-annual scale and consequently failure in producing long-term hydrological dynamics. Firstly, vegetation structure change rather than physiological processes has not been considered. Conventional hydrological models generally employ physiological-process-based models to calculate AET. These are derived from experimental data obtained from individual leaves and then upscaled to the canopy by replacing the leaf-scale resistances with their assumed canopy-scale counterparts (Schymanski and Or, 2017). Thus, such models still operate on a short-term scale, in which AET is sensitive to environmental turbulent diffusion (characterized by weather data) and vegetation physiological processes (e.g., leaf expansion and abscission) (Chen et al., 2022). However, alongside the spatial scaling up, vegetation structure change, such as growth and morality, takes over the priority in influencing AET. This process often takes several years but is ignored in conventional hydrological models. Secondly, the change of soil-water-holding capacity has not been included. Conventional hydrological models typically assume unvary-

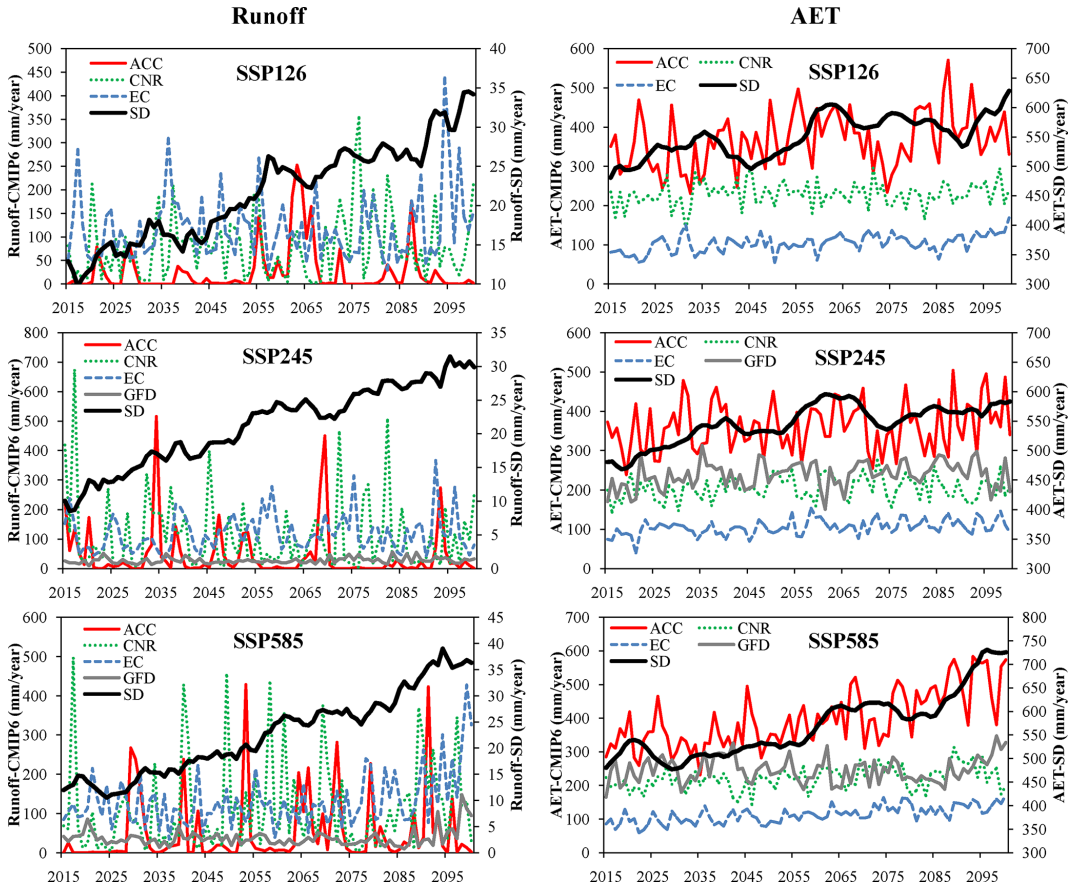

Figure 7. Future runoff and AET predicted by the system dynamics approach under three climatic scenarios and their comparison with predictions from four GCMs. All the dynamics were simulated with fixed ESMS and without human interventions (GP and VEG = 0).

ing soil characteristics and thus stable soil-water-holding capacity. As the soil structural characteristics change slowly, it is permissible to disregard such changes during simulation when the time span is less than decades. However, these changes become discernible at an inter-decadal scale, thereby necessitating the consideration of alterations in soil structural characteristics.

4.2 Advantages and limitations of the system dynamics approach

Firstly, the system dynamics' model in our study is a simplified representation of the complex reality. We argue that both scientific and developmental merits are involved in the proposed model. In essence, the model is a "toy" model. Toy models are frequently used in theoretical physics and many advanced research scopes (Georgescu, 2012). This is because complex systems usually involve a vast number of interacting elements; however, it is often the case that a small number of factors are quantitatively more significant than the others. Therefore, our simplified model only includes key factors providing a good starting point for building a more complex model (Luczak, 2017). The toy model can help us understand a complex system in its broadest strokes. By breaking it down and then building it back up, we gain profound insights into the system's essence.

By adopting the combined structure of a vegetation reinforcing feedback and a soil water–vegetation balancing feedback, our model significantly outperforms traditional rainfall-runoff models and large models at the long-term scale, while demonstrating marginally inferior performance compared to them at the short-term scale. On the one hand, a comparison between our model and SIMHYD, a widely used rainfall-runoff model in Australia (Chiew et al., 2002), was conducted in the Fuping catchment as an example. Monthly rainfall and potential evapotranspiration were used as inputs to the SIMHYD model, and monthly results were aggregated to annual values. Then, an empirical model decomposition method was applied using MATLAB to quantify the performance of both models on short-term and long-term scales (Fig. S13). Results showed that the SIMHYD model only surpassed our model in the short-term Q simulation but performed poorly in the short-term ΔS simulation and long-term AET, Q, and ΔS simulation. On the other hand, previous studies have evaluated runoff simulation from global cli-

mate models (GCMs), global hydrological models (GHMs), and land surface models (LSMs). Results showed that all models performed well in the mean annual Q simulation but struggled with the simulation of inter-annual Q change, with median correlation coefficients (r) close to 0 for GCMs and around 0.6 for GHMs and LSMs (R^2 values ranging from 0.5–0.6) (Zhou et al., 2012; Hou et al., 2023). Given the study context, our model, with R^2 values of 0.23 for Q and 0.7 for other variables at the long-term scale (Fig. S13), exhibits comparable performance to the large models, while requiring significantly fewer data and less computational time.

In the future, our model can be improved from at least two aspects. On the one hand, the mechanism of low hierarchy in the hydrological system can be integrated into the endogenous linking structure to enhance the model's performance at the short-term scale. As discussed earlier, the interaction between rainfall density and sink-filling/macropore flows controls the hydrological behaviors at the intra-annual scale. Thus, high-temporal-resolution rainfall data and detailed soil properties of the topsoil layer are needed to determine the initiation and duration of short-term runoff events. In addition, to link the two hierarchies, intra- and inter-annual, together, soil macropores/sinks should be modeled as dynamic features that evolve in response to vegetation changes. Previous studies showed that the change of plant productivity affects the input of plant products (above- and belowground litter), causing changes in fractions of particulate organic carbon (Shi et al., 2024), subsequently affecting soil-water-holding capacity and storage–discharge relationship. Furthermore, as topsoil texture becomes finer or coarser, water infiltrating into the deep soil changes, which in turn affects vegetation physiology and structure across scales (Wankmüller et al., 2024). On the other hand, the parameter values should be allowed to vary over time rather than being fixed to improve model's performance at the long-term scale. For instance, the fixed utilization ratio of soil water (C2 in Eq. 8) implies that AET solely depends on vegetation coverage and soil bound water but not on plant species. However, the dominant plant species in the study area have shifted from herbs to shrubs due to the implementation of afforestation projects (Liu et al., 2011), resulting in significant changes in the utilization ratio of soil water (Liu et al., 2014). By incorporating variable parameters, the model's performance can be enhanced, as the input of high-quality vegetation data, including vegetation coverage and plant species over time, is actually equivalent to the input of AET based on the intrinsically close links between the two factors.

Secondly, ESMS (Eq. 6) as an important parameter represents the soil-water-holding capacity with value ranging from field capacity to wilting point. Thus, accurate estimation of ESMS is crucial for gaining insights into the long-term hydrological behaviors. However, ESMS is difficult to scale up from field measurements as belowground characteristics, such as soil depth and soil porosity, exhibit high heterogeneity and are not readily observable across a catchment. Moreover, field measurements are often labor-intensive, constrained by space and depth limitations. Thus ESMS estimation remains a significant challenge in hydrology. In our study area, soil characteristics are sparsely observed (Fu et al., 2021), and the results obtained from limited soil samples have a strong bias against the plausible distribution. Furthermore, soil structural characteristics undergo gradual changes over time due to the intricate interplay of soil physical, chemical and biological components. Often, field measurement scales are significantly smaller than the scales relevant to changes in soil structural characteristics.

To address these challenges, this study introduced a "top-down" methodology to estimate ESMS, yet, grounded in the system dynamics principles. Following the exogenous interventions, a dynamical system evolves over time, with its trajectories repeatedly passing through a fixed point or multiple points called the "attractor" (Rickles et al., 2007). In this context, ESMS can be considered the attractor of the hydrological system, which can be inferred from the trajectories of hydrological system dynamics. It is noteworthy that the ESMS is changeable in our study, as the factors that determine ESMS have evolved in tandem with climate change, corresponding to multiple attractors. Previous studies have also suggested that vegetation matrices, such as gross primary productivity (GPP) and leaf area index (LAI), can serve as surrogates for soil structure modifications and soil hydraulic properties (Jha et al., 2023). Although vegetation is still considered an exogenous driver in that framework, these studies highlight the intricate interactions among vegetation, soil structure, and soil moisture.

Finally, the model was developed for a study area characterized by a semi-arid climate with limited water resources. In such regions, energy (temperature and light) is typically abundant and does not constrain vegetation growth. Despite the higher evaporative demand resulting from hotter and drier atmospheric conditions, lack of water hinders the increase in AET by drying out the soil surface, weakening the vegetation, or even causing vegetation death to decrease AET. Therefore, the energy factors such as temperature and light are omitted in our model as the model aims to capture the most critical mechanism in the study area. The success of the model in replicating nonlinear hydrological dynamics proves that the core factors have been identified. However, for regions with energy limitation, such as the high latitudes and the tropics, energy factors could serve as the primary factors, and the soil water–vegetation interaction should be modified into the interaction between energy (temperature/light) and vegetation.

5 Conclusions

Using wavelet analysis, Granger's causality test, and ultimately the system dynamics approach for the headwater of Baiyang Lake in China as an example, this study proposed a

new modeling approach to describe the mechanism of the slow variation of a hydrological system at inter-annual to inter-decadal scales based on four observed variables (P, AET, Q, and ΔS) during the period of 1982–2015. Holistic and insightful understanding was achieved on how a hydrological system functions slowly, as summarized below:

1. Correlation analysis in terms of wavelet coefficients showed that there were constantly negative correlations between AET and the ΔS regardless of climatic periodicity. Meanwhile, the correlations between the two factors and other variables differed in wet and dry phases; for instance, Q was significantly and positively correlated to the ΔS in the wet phase and lost the link in the dry phase. This implies that interconnections between the AET and the ΔS were robust, while the relationships between the two factors and other variables were changing over time.

2. Causal analysis showed a bidirectional causal relationship between AET and ΔS, suggesting the existence of a confounding factor and suggesting that soil water serves as a "confounder" in this relationship. Thus, the causal relationship was subgrouped according to soil water: AET played a dominant role in driving ΔS under plentiful soil water, whereas ΔS determined AET under a lack of soil water.

3. The system dynamics approach built an endogenous linking structure among stocks, which comprised a reinforcing feedback representing the vegetation structure change, and a balancing feedback representing the soil water–vegetation relationship. The structure successfully captured the slow behaviors of a hydrological system at inter-annual to inter-decadal scales under both natural and human-intervention scenarios. Our results showed that at an inter-annual scale, the interaction between the vegetation structure change and the soil bound water dominated the hydrological processes, while at an inter-decadal scale, the interaction between the climatic oscillation and soil-water-holding capacity controlled the hydrological processes.

In conclusion, the system dynamics approach provides a hierarchical view to understand endogenous linking structure of a hydrological system and has the potential to better reproduce the slow hydrological processes at inter-annual to inter-decadal scales compared to conventional hydrological models. With these insights into the hydrological system, we could advance our knowledge in hydrological science in the century of complexity.

Data availability. The gridded data are available in the main text (ETWatch: http://etwatch.cn/html/datasetdatail.html?id=33333a2bee794dac99bc22ec626f430d, ETWatch, 2025a; http://etwatch.cn/html/datasetdatail.html?id=79f37dea8d0c42cf82390bf0a94a59e7, ETWatch, 2025b; NTSG: https://www.umt.edu/numerical-terradynamic-simulation-group/project/global-et.php, NTSG, 2025; CR: https://doi.org/10.11888/AtmosPhys.tpe.249493.file, TPDC, 2022; PEW: https://doi.org/10.11888/Terre.tpdc.272874, TPDC, 2023; TWSA: https://doi.org/10.5061/dryad.z612jm6bt, DRYAD, 2021; ESA CCI: https://climate.esa.int/en/data/#/dashboard, ESA CCI, 2025; CMIP6: https://esgf-node.llnl.gov/search/cmip6/, ESGF MetaGrid, 2025) and the catchment-scale data can be obtained by contacting Xinyao Zhou (zhouxy@sjziam.ac.cn) and Yonghui Yang (yonghui.yang@sjziam.ac.cn).

Supplement. The supplement related to this article is available online at: https://doi.org/10.5194/hess-29-159-2025-supplement.

Author contributions. XZ: conceptualization, methodology, visualization, writing (original draft preparation). ZS and KM: methodology, supervision, writing (review and editing). RZ, QZ, YaY, SH, and JL: resources. YoY: supervision, writing (review and editing).

Competing interests. The contact author has declared that none of the authors has any competing interests.

Disclaimer. Publisher's note: Copernicus Publications remains neutral with regard to jurisdictional claims made in the text, published maps, institutional affiliations, or any other geographical representation in this paper. While Copernicus Publications makes every effort to include appropriate place names, the final responsibility lies with the authors.

Acknowledgements. We would like to thank the three anonymous referees for their insightful suggestions and constructive criticism that have helped us to improve the manuscript greatly.

Financial support. This work was supported by two grants of the National Natural Science Foundation of China (grant nos. 42301036 and 42171046) and the Open Project Program for Hebei Province Collaborative Innovation Center for Sustainable Utilization of Water Resources and Optimization of Industrial Structure (grant no. XTZX202101).

Review statement. This paper was edited by Yongping Wei and reviewed by three anonymous referees.

References

Bai, Y., Langarudi, S. P., and Fernald, A. G.: System dynamics modeling for evaluating regional hydrologic and economic effects of irrigation efficiency policy, Hydrology, 8, 61, https://doi.org/10.3390/hydrology8020061, 2021.

Bailey, V. L., Pries, C. H., and Lajtha, K.: What do we know about soil carbon destabilization?, Environ. Res. Lett., 14, 083004, https://iopscience.iop.org/article/10.1088/1748-9326/ab2c11 (last access: 9 January 2025), 2019.

Banerjee, A., Chandra, S., and Ott, E.: Network inference from short, noisy, low time-resolution, partial measurements: Application to C. elegans neuronal calcium dynamics, P. Natl. Acad. Sci. USA, 120, e2216030120, https://doi.org/10.1073/pnas.2216030120, 2023.

Bouaziz, L., Weerts, A., Schellekens, J., Sprokkereef, E., Stam, J., Savenije, H., and Hrachowitz, M.: Redressing the balance: quantifying net intercatchment groundwater flows, Hydrol. Earth Syst. Sci., 22, 6415–6434, https://doi.org/10.5194/hess-22-6415-2018, 2018.

Bouaziz, L. J. E., Fenicia, F., Thirel, G., de Boer-Euser, T., Buitink, J., Brauer, C. C., De Niel, J., Dewals, B. J., Drogue, G., Grelier, B., Melsen, L. A., Moustakas, S., Nossent, J., Pereira, F., Sprokkereef, E., Stam, J., Weerts, A. H., Willems, P., Savenije, H. H. G., and Hrachowitz, M.: Behind the scenes of streamflow model performance, Hydrol. Earth Syst. Sci., 25, 1069–1095, https://doi.org/10.5194/hess-25-1069-2021, 2021.

Bruelheide, H., Dengler, J., Purschke, O., Lenoir, J., Jimenez-Alfaro, B., Hennekens, S. M., Botta-Dukat, Z., Chytry, M., Field, R., Jansen, F., Kattge, J., Pillar, V. D., Schrodt, F., Mahecha, M. D., Peet, R. K., Sandel, B., van Bodegom, P., Altman, J., Alvarez-Davila, E., Khan, M. A. S. A., Attorre, F., Aubin, I., Baraloto, C., Barroso, J. G., Bauters, M., Bergmeier, E., Biurrun, I., Bjorkman, A. D., Blonder, B., Carni, A., Cayuela, L., Cerny, T., Cornelissen, J. H. C., Craven, D., Dainese, M., Derroire, G., Sanctis, M. D., Diaz, S., Dolezal, J., Farfan-Rios, W., Feldpausch, T. R., Fenton, N. J., Garnier, E., Guerin, G. R., Gutierrez, A. G., Haider, S., Hattab, T. Henry, G., Herault, B., Higuchi, P., Holzel, N., Homeier, J., Jentsch, A., Jurgens, N., Kachi, Z., Karger, D. N., Kessler, M., Kleyer, M., Knollova, I., Korolyuk, A. Y., Kuhn, I., Laughlin, D. C., Lens, F., Loos, J., Louault, F., Lyubenova, M. I., Malhi, Y., Marceno, C., Mencuccini, M., Muller, J. V., Munzinger, J., Myers-Smith, I. H., Neill, D. A., Niinemets, U., Orwin, K. H., Ozinga, W. A., Penuelas, J., Perez-Haase, A., Petrik, P., Phillips, O. L., Partel, M., Reich, P. B., Romermann, C., Rodrigues, A. V., Sabatini, F. M., Sardans, J., Schmidt, M., Seidler, G., Espejo, J. E. S., Silveira, M., Smyth, A., Sporbert, M., Svenning, J.-C., Tang, Z., Thomas, R., Tsiripidis, I., Vassilev, K., Violle, C., Virtanen, R., Weiher, E., Welk, E., Wesche, K., Winter, M., Wirth, C., and Jandt, U.: Global trait-environment relationships of plant communities, Nat. Ecol. Evol., 2, 1906–1917, https://doi.org/10.1038/s41559-018-0699-8, 2018.

Cao, J., Yang, H., and Zhao, Y.: Experimental analysis of infiltration process and hydraulic properties in soil and rock profile in the Taihang Mountain, North China, Water Supply, 22, 1691–1703, https://doi.org/10.2166/ws.2021.321, 2022.

Chaffaut, Q., Hinderer, J., Masson, F., Viville, D., Pasquet, S., Boy, J. P., Bernard, J. D., Lesparre, N., and Pierret, M. C.: New insights on water storage dynamics in a mountainous catchment from superconducting gravimetry, Geophys. J. Int., 228, 432–446, https://doi.org/10.1093/gji/ggab328, 2022.

Chang, L. and Niu, G.: The impacts of interannual climate variability on the declining trend in terrestrial water storage over the Tigris-Euphrates River Basins, J. Hydrometeorol., 24, 549–560, https://doi.org/10.1175/JHM-D-22-0026.1, 2023.

Chen, H., Huang, J. J., Dash, S. S., Wei, Y., and Li, H.: A hybrid deep learning framework with physical process description for simulation of evapotranspiration, J. Hydrol., 606, 127422, https://doi.org/10.1016/j.jhydrol.2021.127422, 2022.

Chen, J., Wilson, C. R., Tapley, B. D., Scanlon, B., and Güntner, A.: Long-term groundwater storage change in Victoria, Australia from satellite gravity and in situ observations, Global Planet. Change, 139, 56–65, https://doi.org/10.1016/j.gloplacha.2016.01.002, 2016.

Chiew, F. H. S., Peel, M. C., and Western, A. W.: Application and testing of the simple rainfall-runoff model SIMHYD, edited by: Singh, V. P., and Frevert, D. K., Mathematical Models of Small Watershed Hydrology and Applications, Water Resources Publication, Littleton, Colorado, 335–367, ISBN 1-887201-35-1, 2002.

Craine, J. M. and Dybzinski, R.: Mechanisms of plant competition for nutrients, water and light, Funct. Ecol., 27, 833–840, https://doi.org/10.1111/1365-2435.12081, 2013.

Creutzfeldt, B., Ferré, T., Troch, P., Merz, B., Wziontek, H., and Güntner, A.: Total water storage dynamics in response to climate variability and extremes: Inference from long-term terrestrial gravity measurement, J. Geophys. Res., 117, D08112, https://doi.org/10.1029/2011JD016472, 2012.

Cui, H., Xiao, W., Zhou, Y., Chen, Y., and Lu, F.: Runoff responses to climate change and human activities in the upper Daqing River Basin, South-to-North Water Transfers and Water Science & Technology, 17, 54–62, https://doi.org/10.13476/j.cnki.nsbdqk.2019.0084, 2019 (in Chinese).

Davis, G. B.: Systems Approach, Encyclopedia of Information Systems, 2003, 351–360, https://doi.org/10.1016/B0-12-227240-4/00178-7, 2003.

Delgado, A. and Gómez, J. A.: The soil. Physical, chemical and biological properties, in: Principles of Agronomy for Sustainable Agriculture, edited by: Villalobos, F. J. and Fereres, E., Springer Cham, Cordoba, Spain, 15–26, https://doi.org/10.1007/978-3-319-46116-8_2, 2016.

Dorigo, W., Wagner, W., Albergel, C., Albrecht, F., Balsamo, G., Brocca, L., Chung, D., Ertl, M., Forkel, M., Gruber, A., Haas, E., Hamer,P.D., Hirschi, M., Ikonen, J., de Jeu, R., Kidd, R., Lahoz, W., Liu, Y.Y., Miralles, D., Mistelbauer, T., Nicolai-Shaw, N., Parinussa, R., Pratola, C., Reimer, C., van der Schalie, R., Seneviratne, S.I., Smolander, T., and Lecomte, P.: ESA CCI Soil Moisture for improved Earth system understanding: State-of-the art and future directions, Remote Sens. Environ., 203, 185–215, https://doi.org/10.1016/j.rse.2017.07.001, 2017.

DRYAD: Data from: Long-term (1979-present) total water storage anomalies over the global land derived by reconstructing GRACE data, DRYAD [data set], https://doi.org/10.5061/dryad.z612jm6bt, 2021.

ESA CCI: ESA soil moisture climate change initiative (soil_moisture_cci): combined prodect, version 06.1, ESA Climate Office [data set], https://climate.esa.int/en/data/#/dashboard, last access: 9 January 2025.

ESGF MetaGrid: CMIP6, ESGF [data set], https://esgf-node.llnl.gov/search/cmip6/, last access: 9 January 2025.

ETWatch: Haihe Basin ET Dataset, ETWatch [data set], http://etwatch.cn/html/datasetdatail.html?id=

33333a2bee794dac99bc22ec626f430d, last access: 9 January 2025a.

ETWatch: Haihe Basin Landuse, ETWatch [data set], http://etwatch.cn/html/datasetdatail.html?id=79f37dea8d0c42cf82390bf0a94a59e7, last access: 9 January 2025b.

Fowler, K., Peel, M., Western, A., Zhang, L., and Peterson, T. J.: Simulating runoff under changing climatic conditions: Revisiting an apparent deficiency of conceptual rainfall-runoff models, Water Resour. Res., 52, 1820–1846, https://doi.org/10.1002/2015WR018068, 2016.

Fowler, K., Pell, M., Western, A., and Zhang, L: Improved rainfall-runoff calibration for drying climate: Choice of objective function, Water Resour. Res., 54, 3392–3408, https://doi.org/10.1029/2017WR022466, 2018.

Fowler, K., Knoben, W., Peel, M., Peterson, T., Ryu, D., Saft, M., Seo, K.-W., and Western, A.: Many commonly used rainfall-runoff models lack long, slow dynamics: Implications for runoff projections, Water Resour. Res., 56, e2019WR025286, https://doi.org/10.1029/2019WR025286, 2020.

Fowler, K. J. A., Coxon, G., Freer, J. E., Knoben, W. J. M., Peel, M. C., Wagener, T., Western, A. W., Woods, R. A., and Zhang, L.: Towards more realistic runoff projections by removing limits on simulated soil moisture deficit, J. Hydrol., 600, 126505, https://doi.org/10.1016/j.jhydrol.2021.126505, 2021.

Forrester, J. W. (Eds.): Principles of Systems, Pegasus Communications Publications, Waltham, MA, ISBN 1883823412, 1968.

Fu, J. and Wang, W.: Global PEW Land Evapotranspiration Data Set (1982–2018), National Tibetan Plateau/Third Pole Environment Data Center [data set], https://doi.org/10.11888/Terre.tpdc.272874, 2022.

Fu, J., Wang, W., Shao, Q., Xing, W., Cao, M., Wei, J., Chen Z., and Nie, W.: Improved global evapotranspiration estimates using proportionality hypothesis-based water balance constraints, Remote Sensing Environ., 279, 113140, https://doi.org/10.1016/j.rse.2022.113140, 2022.

Fu, T., Gao, H., Liang, H., and Liu, J.: Controlling factors of soil saturated hydraulic conductivity in Taihang Mountain Region, northern China, Geoderma Reg., 26, e00417, https://doi.org/10.1016/j.geodrs.2021.e00417, 2021.

Fu, T., Liu, J., Gao, H., Qi, F., Wang, F., and Zhang, M.: Surface and subsurface runoff generation processes and their influencing factors on a hillslope in northern China, Sci. Total Environ., 906, 167372, https://doi.org/10.1016/j.scitotenv.2023.167372, 2024.

Georgescu, I.: Toy model, Nat. Phys., 8, 444, https://doi.org/10.1038/nphys2340, 2012.

Gong, H., Pan, Y., Zheng, L., Li, X., Zhu, L., Zhang, C., Huang, Z., Li, Z., Wang, H., and Zhou, C.: Long-term groundwater storage changes and land subsidence development in the North China Plain, Hydrogeol. J., 26, 1417–1427, https://doi.org/10.1007/s10040-018-1768-4, 2018.

Good, S. P., Noone, D., and Bowen, G.: Hydrologic connectivity constrains partitioning of global terrestrial water fluxes, Science, 349, 175–177, https://doi.org/10.1126/science.aaa5931, 2015.

Han, Q., Tong, R., Sun, W., Zhao, Y., Yu, J., Wang, G., Shrestha, S., and Jin, Y.: Anthropogenic influences on the water quality of the Baiyangdian Lake in North China over the last decade, Sci. Total Environ., 701, 134929, https://doi.org/10.1016/j.scitotenv.2019.134929, 2020.

Hofkirchner, W. and Schafranek, M.: General System Theory, in: Volume 10 in Handbook of the Philosophy of Science, Philosophy of complex systems, edited by: Cliff Hooker, North-Holland, 177–194, https://doi.org/10.1016/B978-0-444-52076-0.50006-7, 2011.

Hou, Y., Guo, H., Yang, Y., and Liu, W.: Global evaluation of runoff simulation from climate, hydrological and land surface models, Water Resour. Res., 59, e2021WR031817, https://doi.org/10.1029/2021WR031817, 2023.

Hu, S., Liu, C., Zheng, H., Wang, Z., and Yu, J.: Assessing the impacts of climate variability and human activities on streamflow in the water source area of Baiyangdian Lake, J. Geogr. Sci., 22, 895–905, https://doi.org/10.1007/s11442-012-0971-9, 2012.

Hu, S., Wang, F., Zhan, C., Zhao, R., Mo, X., and Liu, L.: Detecting and attributing vegetation changes in Taihang Mountain, China, J. Mt. Sci., 16, 337–350, https://doi.org/10.1007/s11629-018-4995-1, 2019.

Hu, Y., Zhai, H., and Tian, Y.: Analysis on sustainability of Taihang Mountain Greening Program construction, Forestry Economics, 2017, 48–52, https://doi.org/10.13843/j.cnki.lyjj.2017.09.009, 2017 (in Chinese).

Huang, C.-C. and Yeh, H.-F.: Evaluation of seasonal catchment dynamic storage components using an analytical streamflow duration curve model, Sustain. Environ. Res., 32, 49, https://doi.org/10.1186/s42834-022-00161-8, 2022.

Huang, Z., Yuan, X., Sun, S., Leng, G., and Tang, Q.: Groundwater depletion rate over China during 1965–2016: The long-term trend and inter-annual variation, J. Geophys. Res-Atmos., 128, e2022JD038109, https://doi.org/10.1029/2022JD038109, 2023.

Hughes, J. D., Petrone, K. C., and Silberstein, R. P.: Drought, groundwater storage and stream flow decline in southwestern Australia, Geophys. Res. Lett., 39, L03408, https://doi.org/10.1029/2011GL050797, 2012.

Hulsman, P., Hrachowitz, M., and Savenije, H. H. G.: Improving the representation of long-term storage variations with conceptual hydrological models in data-scarce regions, Water Resour. Res., 57, e2020WR028837, https://doi.org/10.1029/2020WR028837, 2021.

Jha, A., Bonetti, S., Smith, A. P., Souza, R., and Calabrese, S.: Linking soil structure, hydraulic properties, and organic carbon dynamics: A holistic framework to study the impact of climate change and land management, J. Geophys. Res.-Biogeo., 128, e2023JG007389, https://doi.org/10.1029/2023JG007389, 2023.

Jutebring Sterte, E., Lidman, F., Lindborg, E., Sjöberg, Y., and Laudon, H.: How catchment characteristics influence hydrological pathways and travel times in a boreal landscape, Hydrol. Earth Syst. Sci., 25, 2133–2158, https://doi.org/10.5194/hess-25-2133-2021, 2021.

Kaiser, M., Kleber, M., and Berhe, A. A.: How air-drying and rewetting modify soil organic matter characteristics: an assessment to improve data interpretation and inference, Soil Biol. Biochem., 80, 324–340, https://doi.org/10.1016/j.soilbio.2014.10.018, 2015.

Kuczera, G., Renard, B., Thyer, M., and Kavetski, D.: There are no hydrological monsters, just models and observations with large uncertainties!, Hydrol. Sci. J., 55, 980–991, https://doi.org/10.1080/02626667.2010.504677, 2010.

Lancia, M., Yao, Y., Andrews, C. B., Wang, W., Kuang, X., Ni, J., Gorelick, S. M., Scanlon, B. R., Wang, Y., and Zheng, C.: The

China groundwater crisis: A mechanistic analysis with implications for global sustainability, Sustainable Horizons, 4, 100042, https://doi.org/10.1016/j.horiz.2022.100042, 2022.

Lauf, S., Haase, D., Hostert, P., Lakes, T., and Kleinschmit, B.: Uncovering land-use dynamics driven by human decision-making – A combined model approach using cellular automata and system dynamics, Environ. Modell. Softw., 27–28, 71–72, https://doi.org/10.1016/j.envsoft.2011.09.005, 2012.

Li, F., Kusche, J., Chao, N., Wang, Z., and Löcher, A.: Long-term (1979–present) total water storage anomalies over the global land derived by reconstructing GRACE data, Geophys. Res. Lett., 48, e2021GL093492, https://doi.org/10.1029/2021GL093492, 2021.

Li, W., Pacheco-Labrador, J., Migliavacca, M., Miralles, D., van Dijke, A. H., Reichstein, M., Forkel, M., Zhang, W., Frankenberg, C., Panwar, A., Zhang, Q., Weber, U., Gentine, P., and Orth, R.: Widespread and complex drought effects on vegetation physiology inferred from space, Nat. Commun., 14, 4640, https://doi.org/10.1038/s41467-023-40226-9, 2023.

Lian, X., Piao, S., Chen, A., Wang, K., Li, X., Buermann, W., Huntingford, C., Peñuelas, J., Xu, H., and Myneni, R. B.: Seasonal biological carryover dominates northern vegetation growth, Nat. Commun., 12, 983, https://doi.org/10.1038/s41467-021-21223-2, 2021.

Liu, X., Zhang, W., Liu, Z., Qu, F., and Tang, X.: Changes in species diversity and above-ground biomass of shrubland over long-term natural restoration process in the Taihang Mountain in North China, Plant Soil Environ., 57, 505–512, https://doi.org/10.17221/216/2011-PSE, 2011.

Liu, X. P., Zhang, W. J., Hu, C. S., and Tang, X. G.: Soil greenhouse gas fluxes from different tree species on Taihang Mountain, North China, Biogeosciences, 11, 1649–1666, https://doi.org/10.5194/bg-11-1649-2014, 2014.

Luczak, J.: Talk about toy models, Stud. Hist. Philos. Sci., 57, 1–7, https://doi.org/10.1016/j.shpsb.2016.11.002, 2017.

Ma, H., Zeng, J., Chen, N., Zhang, X., Cosh, M. H., and Wang, W.: Satellite surface soil moisture from SMAP, SMOS, AMSR2 and ESA CCI: A comprehensive assessment using global ground-based observations, Remote Sens. Environ., 231, 111215, https://doi.org/10.1016/j.rse.2019.111215, 2019c.

Ma, N., Jozsef, S., Zhang, Y., and Liu, W.: Terrestrial evapotranspiration dataset across China (1982–2017), National Tibetan Plateau/Third Pole Environment Data Center [data set], https://doi.org/10.11888/AtmosPhys.tpe.249493.file, 2019a.

Ma, N., Szilagyi, J., Zhang, Y. S., and Liu, W. B.: Complementary-relationship-based modeling of terrestrial evapotranspiration across China during 1982–2012: Validations and spatiotemporal analyses, J. Geophys. Res-Atmos., 124, 4326–4351, https://doi.org/10.1029/2018JD029850, 2019b.

Manzoni, S., Chakrawal, A., Fischer, T., Schimel, J. P., Porporato, A., and Vico, G.: Rainfall intensification increases the contribution of rewetting pulses to soil heterotrophic respiration, Biogeosciences, 17, 4007–4023, https://doi.org/10.5194/bg-17-4007-2020, 2020.

Markovich, K. H., Maxwell, R. M., and Fogg, G. E.: Hydrogeological response to climate change in alpine hillslopes, Hydrol. Process., 30, 3126–3138, https://doi.org/10.1002/hyp.10851, 2016.

McDonnell, J. J., Spence, C., Karran, D. J., van Meerveld, H. J., and Harman, C. J.: Fill-and Spill: A process description of runoff generation at the scale of the beholder, Water Resour. Res., 57, e2020WR027514, https://doi.org/10.1029/2020WR027514, 2021.

Meadows, D. H. (Eds.): Thinking in Systems: A Primer, Chelsea Green Publishing, ISBN 9781603581486, 2008.

Moiwo, J. P., Yang, Y., Yan, N., and Wu, B.: Comparison of evapotranspiration estimated by ETWatch with that derived from combined GRACE and measured precipitation data in Hai River Basin, North China, Hydrol. Sci. J., 56, 249–267, https://doi.org/10.1080/02626667.2011.553617, 2011.

Morgan, S. L. and Winship, C. (Eds.): Counterfactuals and causal inference: Methods and Principles for social research, 2nd edn., Cambridge University Press, Cambridge, UK, ISBN 9781107694163, 2015.

Nalley, D., Adamowski, J., Khalil, B., and Biswas, A.: Inter-annual to inter-decadal streamflow variability in Quebec and Ontario in relation to dominant large-scale climate indices, J. Hydrol., 536, 426–446, https://doi.org/10.1016/j.jhydrol.2016.02.049, 2016.

Negassa, W. C., Guber, A. K., Kravchenko, A. N., Marsh, T. L., Hildebrandt, B., and Rivers, M. L.: Properties of soil pore space regulate pathways of plant residue decomposition and community structure of associated bacteria, PLoS ONE, 10, 1–22, https://doi.org/10.1371/journal.pone.0123999, 2015.

NTSG: Global ET, University of Montana [data set], https://www.umt.edu/numerical-terradynamic-simulation-group/project/global-et.php, last access: 9 January 2025.

O'Connell, P. E., Koutsoyiannis, D., Lins, H. F., Markonis, Y., Montanari, A., and Cohn, T. A.: The scientific legacy of Harold Edwin Hurst (1880–1978), Hydrol. Sci. J., 61, 1571–1590, https://doi.org/10.1080/02626667.2015.1125998, 2016.

Patel, K. F., Fansler, S. J., Compbell, T. P., Bond-Lamberty, B., Smith, A. P., RoyChowdhury, T., McCue, L. A., Varga, T., and Bailey, V. L.: Soil texture and environmental conditions influence the biogeochemical responses of soils to drought and flooding, Commun. Earth Environ., 2, 127, https://doi.org/10.1038/s43247-021-00198-4, 2021.

Pathak, R. S. (Eds.): The wavelet transform (Atlantis Studies in Mathematics for Engineering and Science), AP/World Scientific Publishing, Paris, France, 192 pp., ISBN 9078677260, 2009.

Pearl, J. (Eds.): Causality: Models, reasoning, and inference, 2nd edn., Cambridge University Press, Cambridge, UK, ISBN 052189560X, 2009.

Richardson, G. P.: Core of System Dynamics, in: System Dynamics. Envyclopedia of Complexity and System Science Series, edited by: Dangerfield, B., Springer, New York, NY, 11–20, https://doi.org/10.1007/978-1-4939-8790-0_536, 2020.

Rickles, D., Hawe, P., and Shiell, A.: A simple guide to chaos and complexity, J. Epidemiol. Commun. H., 61, 933–937, https://doi.org/10.1136/jech.2006.054254, 2007.

Peterson, T. J., Saft, M., Peel, M. C., and John, A.: Watersheds may not recover from drought, Science, 372, 745–749, https://doi.org/10.1126/science.abd5085, 2021.

Robert: Granger_Cause_1, MATLAB Central File Exchange [code], https://www.mathworks.com/matlabcentral/fileexchange/59390-granger_cause_1 (last access: 9 January 2025), 2023.

Sayood, K.: Wavelets, in: Introduction to Data Compression, the Morgan Kaufmann Series in Multimedia Information and Systems, Morgan Kaufmann, 497–528, https://doi.org/10.1016/B978-0-12-415796-5.00015-6, 2012.

Schymanski, S. J. and Or, D.: Leaf-scale experiments reveal an important omission in the Penman–Monteith equation, Hydrol. Earth Syst. Sci., 21, 685–706, https://doi.org/10.5194/hess-21-685-2017, 2017.

Seth, A. K. and Bayne, T.: Theories of consciousness, Nat. Rev. Neurosci., 23, 439–452, https://doi.org/10.1038/s41583-022-00587-4, 2022.

Shi, B., Delgado-Baquerizo, M., Knapp, A. K., Smith, M. D., Reed, S., Osborne, B., Carrillo, Y., Maestre, F. T., Zhu, Y., Chen, A., Wilkins, K., Holdrege, M. C., Kulmatiski, A., Picon-Cochard, C., Roscher, C., Power, S., Byrne, K. M., Churchill, A. C., Jentsch, A., Henry, H. A. L., Beard, K. H., Schuchardt, M. A., Elsenhauer, N., Otfinowski, R., Hautler, Y., Shen, H., Wang, Y., Wang, Z., Wang, C., Cusack, D. F., Petraglla, A., Carbognani, M., Forte, T. G. W., Flory, S., Hou, P., Zhang, T., Gao, W., and Sun, W.: Aridity drives the response of soil total and particulate organic carbon to drought in temperate grasslands and shrublands, Sci. Adv., 10, eadq2654, https://doi.org/10.1126/sciadv.adq2654, 2024.

Shi, H., Zhao, Y., Liu, S., Cai, H., and Zhou, Z.: A new perspective on drought propagation: causality, Geophys. Res. Lett., 49, e2021GL096758, https://doi.org/10.1029/2021GL096758, 2022.

Simonovic, S. P.: Application of the systems approach to the management of complex water systems, Water, 12, 2923, https://doi.org/10.3390/w12102923, 2020.

Snider, S. B. and Brimlow, J. N.: An introduction to population growth, Nature Education Knowledge, 4, 3, https://www.nature.com/scitable/knowledge/library/an-introduction-to-population-growth-84225544/ (last access: 9 January 2025), 2013.

Sterman, J. D. (Eds.): Business Dynamics: System thinking and modeling for a complex world, McGraw-Hill Education, ISBN 9780072389159, 2000.

Su, X., Su, X., Yang, S., Zhou, G., Ni, M., Wang, C., Qin, H., Zhou, X., and Deng, J.: Drought changed soil organic carbon composition and bacterial carbon metabolizing patterns in a subtropical evergreen forest, Sci. Total Environ., 76, 139568, https://doi.org/10.1016/j.scitotenv.2020.139568, 2020.

Sugihara, G., May, R., Ye, H., Hsieh, C., Deyle, E., Fogarty, M., and Munch, S.: Detecting causality in complex ecosystems, Science, 338, 496–500, https://doi.org/10.1126/science.1227079, 2012.

Stokes, P. A. and Purdon, P. L.: A study of problems encountered in Granger causality analysis from a neuroscience perspective, P. Natl. Acad. Sci. USA, 114, E7063–E7072, https://doi.org/10.1073/pnas.1704663114, 2017.

Stocker, B. D., Tumber-Dávlla, S. J., Konlngs, A. G., Anderson, M. C., Hain, C., and Jackson, R. B.: Global patterns of water storage in the rooting zones of vegetation, Nat. Geosci., 16, 250–256, https://doi.org/10.1038/s41561-023-01125-2, 2023.

TPDC: Terrestrial evapotranspiration dataset across China (1982–2017), TPDC [data set], https://doi.org/10.11888/AtmosPhys.tpe.249493.file, 2022.

TPDC: Global PEW land evapotranspiration dataset (1982–2018), TPDC [data set], https://doi.org/10.11888/Terre.tpdc.272874, 2023.

Wang, H., Lv, X., and Zhang, M.: Sensitivity and attribution analysis based on the Budyko hypothesis for streamflow change in Baiyangdian catchment, China, Ecol. Indic., 121, 107221, https://doi.org/10.1016/j.ecolind.2020.107221, 2021.

Wankmüller, F. J. P., Delval, L., Lehmann, P., Baur, M. J., Cecere, A., Wolf, S., Or, D., Javaux, M., and Carminati, A.: Global influence of soil texture on ecosystem water limitation, Nature, 635, 631–638, https://doi.org/10.1038/s41586-024-08089-2, 2024.

Wei, C. and Wang, H.: Research of water supply strategies in Fuping county, Design of Water Resources & Hydroelectric Engineering, 38, 21–23, 2019 (in Chinese).

Wei, J. and Dirmeyer, P. A.: Sensitivity of land precipitation to surface evapotranspiration: a nonlocal perspective based on water vapor transport, Geophys. Res. Lett., 46, 12588–12597, https://doi.org/10.1029/2019GL085613, 2019.

Wiener, N. (Eds.): Cybernetics: or Control and Communication in the Animal and the Machine, John Wiley & Sons, New York, 194 pp., ISBN 9780262355902, 1948.

Wright, A. J. and Francia, R. M.: Plant traits, microclimate temperature and humidity: A research agenda for advancing nature-based solution to a warming and drying climate, J. Ecol., 112, 2462–2470, https://doi.org/10.1111/1365-2745.14313, 2024.

Wu, B., Xiong, J., and Yan, N., Yang, L., and Du, X.: ETWatch for monitor regional evapotranspiration with remote sensing, Advances in Water Science, 19, 671–678, 2008.

Wu, B., Yan, N., Xiong, J., Bastiaanssen, W. G. M., Zhu, W., and Stein, A.: Validation of ETWatch using field measurements at diverse landscapes: A case study in Hai Basin of China, J. Hydrol., 436–437, 67–80, https://doi.org/10.1016/j.jhydrol.2012.02.043, 2012.

Wu, F., Wu, B., Zhu, W., Yan, N., Ma, Z., Wang, L., Lu, Y., and Xu, J.: ETWatch cloud: APIs for regional actual evapotranspiration data generation, Environ. Modell. Softw., 145, 105174, https://doi.org/10.1016/j.envsoft.2021.105174, 2021.

Xiao, D., Shi, Y., Brantley, S. L., Forsythe, B., DiBiase, R., Davis, K., and Li, L.: Streamflow generation from catchments of contrasting lithologies: the role of soil properties, topography, and catchment size, Water Resour. Res., 55, 9234–9257, https://doi.org/10.1029/2018WR023736, 2019.

Xu, Q., Cheng, W., Sun, T., and Bo, Q.: The influence of climate factors on runoff of major rivers in upper reaches of Baiyangdian lake, Journal of Hebei Agricultural University, 42, 110–115, https://doi.org/10.13320/j.cnki.jauh.2019.0043, 2019 (in Chinese).

Yang, H. and Cao, J.: Analysis of basin morphologic characteristics and their influence on the water yield of mountain watersheds upstream of the Xiongan New Area, North China, Water, 13, 2903, https://doi.org/10.3390/w13202903, 2021.

Yang, Z. and Mao, X.: Wetland system network analysis for environmental flow allocations in the Baiyangdian Basin, China, Ecol. Model., 222, 3785–3794, https://doi.org/10.1016/j.ecolmodel.2011.09.013, 2011.

Yuan, Z., Yan, D. H., Xu, J. J., Wang, Y. Q., Yao, L. Q., and Yu, Z. Q.: Effects of the precipitation pattern and vegetation coverage variation on the surface runoff characteristics in the eastern Taihang Mountain, Appl. Ecol. Environ., 17, 5753–5764, https://doi.org/10.15666/aeer/1703_57535764, 2019.

Zera, D. A.: What is a system and a system perspective?, Educ. Horiz., 81, 18–20, http://www.jstor.org/stable/42925422 (last access: 9 January 2025), 2002.

Zeng, Y., Zhao Y., and Qi, Z.: Evaluating the ecological state of Chinese Lake Baiyangdian (BYD) based on

ecological network analysis, Ecol. Indic., 127, 107788, https://doi.org/10.1016/j.ecolind.2021.107788, 2021.

Zhang, K., Kimball, J. S., Mu, Q., Jones, L. A., Goetz, S. J., and Running, S. W.: Satellite based analysis of northern ET trends and associated changes in the regional water balance from 1983 to 2005, J. Hydrol., 379, 92–110, https://doi.org/10.1016/j.jhydrol.2009.09.047, 2009.

Zhang, K., Kimbal, J. S., Nemani, R. R., and Running, S. W.: A continuous satellite-derived global record of land surface evapotranspiration from 1983 to 2006, Water Resour. Res., 46, W09522, https://doi.org/10.1029/2009WR008800, 2010.

Zhang, Q., Shao, M., Jia, X., and Wei, X.: Changes in soil physical and chemical properties after short drought stress in semi-humid forests, Geoderma, 338, 170–177, https://doi.org/10.1016/j.geoderma.2018.11.051, 2019.

Zhao, H., Gao, G., An, W., Zou, X., Li, H., and Hou, M.: Timescale differences between SC-PDSI and SPEI for drought monitoring in China, Phys. Chem. Earth, 102, 48–58, https://doi.org/10.1016/j.pce.2015.10.022, 2017.

Zhou, X., Zhang, Y., Wang, Y., Zhang, H., Vaze, J., Zhang, L., Yang, Y., and Zhou, Y.: Benchmarking global land surface models against the observed mean annual runoff from 150 large basins, J. Hydrol., 470–471, 269–279, https://doi.org/10.1016/j.jhydrol.2012.09.002, 2012.

Zhu, Y., Wang, H., Ma, J., Wang, T., and Sun, J.: Contribution of the phase transition of Pacific Decadal Oscillation to the late 1990s' shift in East China summer rainfall, J. Geophys. Res.-Atmos., 120, 8817–8827, https://doi.org/10.1002/2015JD023545, 2015.

Zhuang, C., Ouyang, Z., Xu, W., Bai, Y., Zhou, W., Zheng, H., and Wang, X.: Impacts of human activities on the hydrology of Baiyangdian Lake, China, Environ. Earth Sci., 62, 1343–1350, https://doi.org/10.1007/s12665-010-0620-5, 2011.